



Highly conductive self-electrical stimuli core-shell conduit based on PVDF-chitosan–gelatin filled with in-situ gellan gum as a possible candidate for nerve regeneration: a rheological, electrical, and structural study

Mojdeh Mohseni^{1,2} · Ahmad Ramazani Saadatabadi³

Received: 3 April 2021 / Accepted: 8 August 2021 / Published online: 17 August 2021
© King Abdulaziz City for Science and Technology 2021

Abstract

In the context of peripheral nerve injuries treatment, self-electrical stimuli nerve guidance conduit is a promising technique. To fabricate such structures, PVDF-chitosan–gelatin was considered for the outside walls of conduit and gellan gum containing conductive polyaniline-graphene (PAG) nanocomposite particles in the middle. PVDF-chitosan–gelatin nanofibers were prepared using the dual-electrospinning method and highly conductive binary-doped polyaniline-graphene was synthesized by chemical oxidative polymerization in the presence of aniline and sodium dodecyl sulfate. The morphology and chemical structure of nanofibers and PAG were characterized using SEM and FTIR analyses. The morphological, structural, electrical, and mechanical properties of gellan containing PAG particles were investigated with SEM, FTIR, piezoelectric and rheology tests. Gelation time, swelling, and degradation of gellan PAG were also studied. Morphological investigation of self-electrical stimuli conduit represents successful electrospinning and the polymerization of polyaniline was confirmed using FTIR and XRD methods. The designed conduit shows the adequate output voltage and highly oriented pore structures in gellan gel as an in-situ thermosensitive construction makes convenient properties for peripheral nerve injury treatment. Our obtained results illustrate that the self-electrical nerve guidance conduit with gellan PAG can provide a novel substrate as a neural conduit.

Keywords Conduit · Gellan · Aniline · Graphene

Introduction

Peripheral nerve injury is a widespread disease caused by trauma, natural disasters, and accident annually, many people suffer from this disservice. The disadvantages of autograph and allograft in peripheral nerve damages approaches such as possible inflammation and disease transmission provide some limitations (Hua et al. 2018). An alternative method for this aim is introduced as a nerve guidance

conduit (NGC). In this technique, the need for secondary surgery is removed and the tunable properties based on host tissue are the main preponderances (Shen et al. 2011).

For NGC designing, electrical conductivity, Physico-chemical adaption with damaged zone, and also texture properties play a crucial role (Zeng et al. 2011). Although, a wide range of conductive materials are candidates for this goal but applying self-electrical stimuli substitute for NGC fabrication can overcome common restrictions (Ming et al. 2018). Poly (vinylidene fluoride) (PVDF) with the piezoelectric behavior under effect on the β -phase formation which is made using planar configuration the dipole moments in a parallel situation, can achieve an electrical environment in NGC without any external stimulations (Badatya et al. 2021).

The presence of other biopolymers specifically natural ones including chitosan and gelatin in the piezoelectric NGC would manage the wettability and cellular interaction with these structures (Yuan-YuHsueh 2014; Liu et al. 2020).

✉ Ahmad Ramazani Saadatabadi
ramazani@sharif.edu

¹ Department of Medical Nanotechnology, Faculty of Advanced Technologies in Medicine, Iran University of Medical Sciences, Tehran, Iran
² Radiation Biology Research Center, Iran University of Medical Sciences, Tehran, Iran
³ Chemical and Petroleum Engineering Department, Sharif University of Technology, Tehran, Iran

Chitosan, a deacetylated form of chitin, with the features of biocompatibility and biodegradability, and gelatin as a protein representative material are suitable substrates for NGC synthesis (Abnoos et al. 2018; Xiao et al. 2021).

Hydrogels recognized as a three-dimensional network with the ability of a high amount of water absorbance are widely implied in various biomedical engineering applications (Ilka et al. 2018). These kinds of materials are used for contact lens (Silva et al. 2021), wound dressing (Zhang and Zhao 2020), and tissue engineering scaffolds (Mohseni and Dezfouli 2020), and with their potential to mimic the extracellular matrix (ECM) of cells and create stiffness resemble living tissues attracted more attentions (Mohseni et al. 2020).

Generally, natural polymers have outstanding virtues and among them, polysaccharides make the possibilities of efficient cellular interaction with tunable chemical and mechanical properties (Maity et al. 2021).

In the wide range of natural biomaterials, carbohydrates have some applicable potentials for biomedicine (Pan et al. 2021). Gellan gum with Food and Drug Administration (FDA) approved, is adopted for hydrogel fabricating (Mohseni et al. 2021a). This polysaccharide is adequate in diverse tissue engineering areas including cartilage (Lee 2020), bone (Lin and Chiu 2020), tendon (Park et al. 2021). But using this structure as an in-situ gel in neural applications is constrained because of the lack of sufficient electrical conductivity of gellan gum (Maharjan 2020).

In the tissue engineering ideology particularly nerve regeneration, electroactive structures such as polymers allow electrical stimulation for functional cell performances (Deval Prasad Bhattarai 2018). Polyaniline (PANI), has been recognized as a conductive polymer for axonal elongation (Gao et al. 2021) has the privileges of environmental stability and high conductivity (Mohseni et al. 2021b). To improve the electrical conductivity of PANI, the presence of other materials with electroactivity such as graphene nano-sheet can produce nanocomposite to control Physico-chemical features of PANI (Bilal Ahmad Farooqi 2020). The nanocomposite of polyaniline-graphene (PAG) overcome the weakness of each compartment individually and the synthesis of this nanocomposite presents better electrical conductivity (Kung 2021; Mohammadi 2020).

Herein, self-electrical stimuli based on PVDF-chitosan-gelatin NGC filled by conductive gellan gum were fabricated. The dual-electrospinning method was used for fiber preparation and the nanocomposite of polyaniline-graphene was synthesized with an in-situ emulsion polymerization method with enhanced conductivity. Physico-chemical features of electrospun piezoelectric nanofibers were characterized using SEM, FTIR, contact angle, and the analyses of PAG structures were FTIR, XRD, and SEM. The rheological behavior of gellan comprising PAG particles was studied

with the help of viscosity, storage, and loss modulus diagrams, and electroactivity of designed neural conduit was measured.

Materials and methods

Materials

Aniline monomer, ammonium peroxydisulfate (APS), sodium dodecyl sulfate (SDS), phosphate-buffered saline (PBS), gellan powder (low acyl), and graphene were obtained from Sigma-Aldrich. Chitosan [poly (D-glucosamine) deacetylated chitin] and gelatin type A (derived from porcine skin, bloom 175 were supplied from Sigma-Aldrich. Poly(vinylidene fluoride) with a molecular weight (Mw) of 270,000 g mol⁻¹, N, N-Dimethylformamide (DMF), glacial acetic acid (99.7% purity) were purchased from Merck (Germany). MTT (3[4,5-dimethylthiazol-2-yl]-2,5-diphenyltetrazolium bromide), and phosphate-buffered saline (PBS), Fetal Bovine Serum (FBS), RPMI 1640 (culture medium), trypsin-EDTA, penicillin-streptomycin were supplied from Sigma-Aldrich.

Electrospinning of PVDF-chitosan-gelatin nanofibers

Piezoelectric-based nanofibers were prepared by the technique of the dual-electrospinning method. For this aim, PVDF solution was prepared by dissolving a specified amount of polymer in DMF at 50 °C. Acetone was added dropwise to dissolved PVDF solution and was magnetic stirred at ambient temperature for 2 h. The proportion of DMF: acetone in this step was considered at 60:40 and the homogenous solution was electrospun with the voltage of 14 kV, the flow rate of 0.5 ml/min, and nozzle-collector distance of 14 cm. The optimum concentration of PVDF was characterized at different concentrations of 5, 70, 10, 15, and 25 (%w/v).

To electrospinning process of PVDF-chitosan-gelatin nanofibers, chitosan solution was prepared by dissolving of polymer in acetic acid 2 (%v/v) and gelatin solution in the solvent of acetic acid 20 (%v/v) at 45 °C was added to the previous solution and stirred for 7 h. Two syringes (chitosan-gelatin solution, PVDF solution) were connected to a high voltage of 19 kV, rotating drum with a speed of 250 rpm and the distance between each needle and collector was 14 cm with the flow rate of 0.5 ml/min were the condition of the electrospinning process. The schematic diagram of chitosan-gelatin-PVDF nanofiber synthesis was shown in Fig. 1.

Three experiments were applied based on Table 1 but the final concentration of chitosan: gelatin for further evaluation

Fig. 1 Scheme of PVDF-chitosan–gelatin nanofibers with dual-electrospinning technique

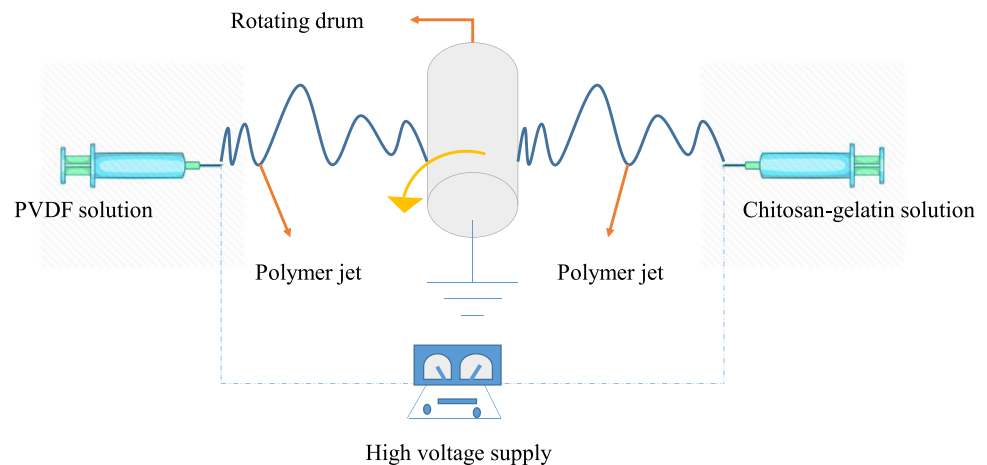


Table 1 Samples with different amount of PAG loading

Chitosan–gelatin (%v/v)	Sample
70:30	GC1
50:50	GC2
30:70	GC3

was 30:70. All solution compositions of chitosan–gelatin were expressed in (%v/v).

Polyaniline-graphene (PAG) nanocomposite

PAG was synthesized using emulsion polymerization (Adrián Magaz et al. 2021). Briefly, 0.5 (wt.%) of graphene was dispersed in HCL (1 M) containing monomer of aniline under ultrasound technique with the power of 80 w for 6 min. Graphene in HCL and monomer was transferred to the three-necked flask in the condition of nitrogen purging and the temperature of 5 °C in ice bath status and 5.767 g SDS was added to the previous mixture under continuous stirring. A fresh solution of APS containing 0.913 g in 10 ml HCL (1 M) was added dropwise to aniline-graphene for 30 min. The polymerization process was continued for 6 h until the color was tuned in to a bluish, the structure was kept at room temperature for 24 h. Methanol, ethanol, and water were used to remove unreacted ingredients several times with a centrifuge device. Finally, dried PAG powder was obtained with maintenance at room temperature for 24 h. The obtained conductive nanocomposites were dispersed in deionized water to prevent any possible aggregations.

Conductive gellan gel

Highly conductive in-situ gellan gel was accomplished by adding PAG nanocomposite to gellan solution. The

procedural steps for the synthesis of conductive thermo-sensitive gels are as follows; First, gellan gum solution was achieved by dissolving the polymeric powder in deionized water at 90 °C magnetically stirring. The gelation mechanism was controlled by 10 µl of 2 (%v/v) acetic acid at the pH of 4.5. Second, a conductive nanocomposite of PAG dispersed in 2 ml deionized water with the help of an ultrasound homogenizer (power 80 w, 10 min) was added during homogenizing the gellan solution at 90 °C. Diverse PAG compositions [1, 1.5, and 2 (wt.%) dispersion was loaded into dissolved gellan solution and was further stirred for 4 h.

Gellan solutions were cross-linked with the use of CaCl₂ [1 (%w/v)] and scaffolds with two approaches were fabricated. In the first one, gellan with the temperature of 90 °C was kept at room temperature to have stable gels and then formed gels were transferred to the freezer (-70 °C) and in the second approach, hot gellan (90 °C) directly moved to -70 °C.

Fabrication of PVDF-based nanofibers filled with gellan PAG

The highly oriented gellan-PAG gel was synthesized using the freeze-drying method. For this purpose, electroactive gel formulations obtained in see “Conductive gellan gel” were poured in a cylindrical tube wrapped with Styrofoam insulation around sidewalls with varied thicknesses of 15 and 25 mm and frozen at -70 °C and freeze-dried. The polymeric networks have been tuned to hydrogels with rehydration in PBS medium.

For fabrication of nerve conduit based on PVDF nanofibers filled gellan PAG, rectangular shape of the electrospun mat (3 × 10 cm²) was rolled around prepared aligned gellan gel containing different amount of PAG nanoparticles.

Characterization

PVDF-chitosan–gelatin nanofibers characterizations

The morphological information of PVDF nanofibers and PVDF-chitosan–gelatin electrospun fibers was obtained via SEM (PHILIPS XL30) device at an accelerating voltage of 25 kV after gold coating using a sputter coater.

For chemical structure identification of electrospun nanofibers, FTIR spectroscopy (Bruker, Ettlingen, Germany) was implied in the range of 3500–500 cm^{-1} .

The wettability of electrospun nanofibers was measured with a contact angle analyzer (SHARIF AZMA, CA-1, Iran). The test was repeated three times and conducted at room temperature.

PAG analyses

The chemical structure of PAG nanocomposite was studied using FTIR (Bruker, Ettlingen, Germany) analysis. The pellet technique with KBr was used and the spectra in the range of 4000–1000 cm^{-1} were captured.

XRD (Unisantis, XMD 300, Germany) analysis was implied for the characterization of the crystalline behavior of PAG. Diffracted peaks in the span of $2\theta = 5\text{--}50^\circ$ were recorded and the device setting was 30 mA and 40 kV for current and voltage respectively.

The morphology of synthesized PAG structures was visualized using SEM (PHILIPS XL30) analysis after gold coating at an accelerating voltage of 20 kV.

Rheology study

The rheological parameters of gellan solution containing PAG have studied with Physica MCR 301 rheometer (Anton Paar) with 25 mm parallel plates. Viscosity, G' , and G'' of samples at diverse frequencies at the temperature of 90 °C were analyzed for 10 min.

Structural study of gellan composite

X-ray diffractometer (XRD) (Equinox 300) analysis was performed for phase detection over a 2θ range of 5–50°. The current and voltage setting of the device was 30 mA and 40 kV respectively.

Electrical properties study

The conductivity of scaffolds was measured with a standard four-point probe. The constant current of 0.5 mA and the room temperature was the condition of the experiment.

Using the recorded voltage, current, and thickness of samples the electrical conductivity of scaffolds was calculated using the following equation:

$$\sigma = \frac{Ln2}{\pi t} \left(\frac{I}{V} \right)$$

where σ is electrical conductivity (S/cm), t is the thickness (cm), I considered as current (A), and V is voltage (V) (Gupta et al. 2006). Each sample was repeated three times and the average value was reported.

The piezoelectric behavior of self-electrical conduit was evaluated using a digital oscilloscope (ROHDE & SCHWARZ, HMO-3522, Germany) at constant force and frequency at ambient temperature.

Gelation time

Based on Gupta et al.'s reports, the gelation time of gellan with different contents of PAG was determined (Jun et al. 2009). Briefly, 2 ml of gellan-based solution was maintained at 90 °C for 5 min and immersed in a vial tube with an inner diameter of 10 mm. Solutions were kept at room temperature and gelation time was specified. The time of gels couldn't flow was set as gelation time.

Biodegradation test

To evaluate the degradation of scaffolds, each sample with a dimension of 1 × 3 cm was prepared and weighed. Samples were immersed in PBS (pH 7.4) and kept in a shaking incubator (temperature of 37 °C) for 30 days. Weight changes of specimens were determined and reported according to the following equation:

$$\text{Degradation (\%)} = (M_1 - M_0) / M_0 \times 100$$

where M_0 is the initial mass and M_1 is the mass of scaffolds after a particular time.

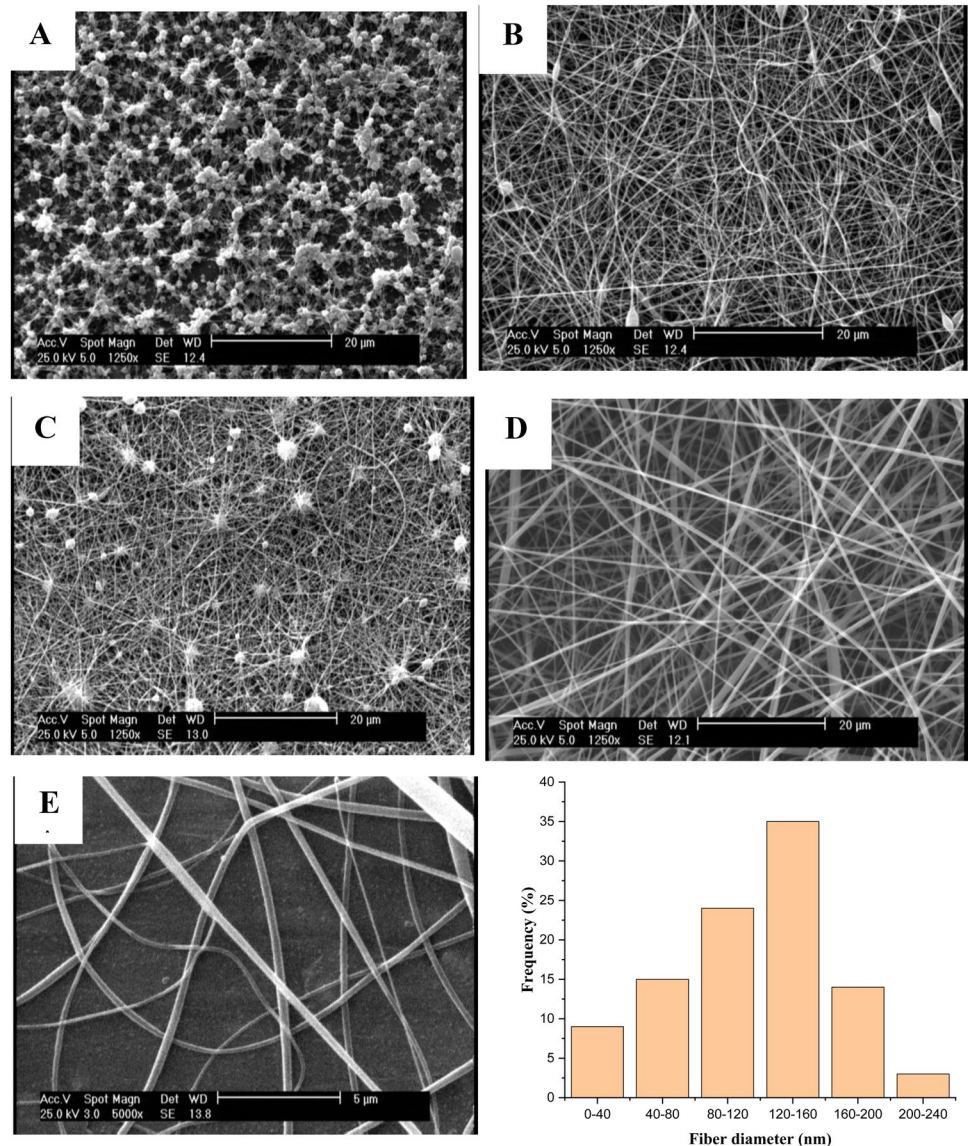
Scaffold swelling

The swelling behavior of gellan-based gels was examined by submerging the specified amount of scaffold in PBS at 37 °C with filter paper, surplus PBS was removed and the weight of swollen and dried scaffolds was recorded. The swelling ratio was calculated wing following equation:

$$\text{Swelling (\%)} = (W_2 - W_1) / W_1 \times 100$$

W_1 is the dried scaffold and W_2 is the weight of the swollen sample.

Fig. 2 SEM images of PVDF nanofibers at different concentration of **A** 5 (%w/v), **B** 7 (%w/v), **C** 10 (%w/v), **D** 15 (%w/v), **E** 25 (%w/v)



In vitro culture of PC12

PC12 cells (neuronal model cells) were obtained from Pastor Institute cell bank. Cells were cultured in a tissue culture flask in RPMI-1640 medium containing penicillin–streptomycin, FBS (10%) at CO₂ (5%), and 37 °C. The culture medium was changed every day and kept in an incubator until cells reach 70% of confluency. Thereafter, cells were detached for MTT assay for cytotoxicity appraisalment.

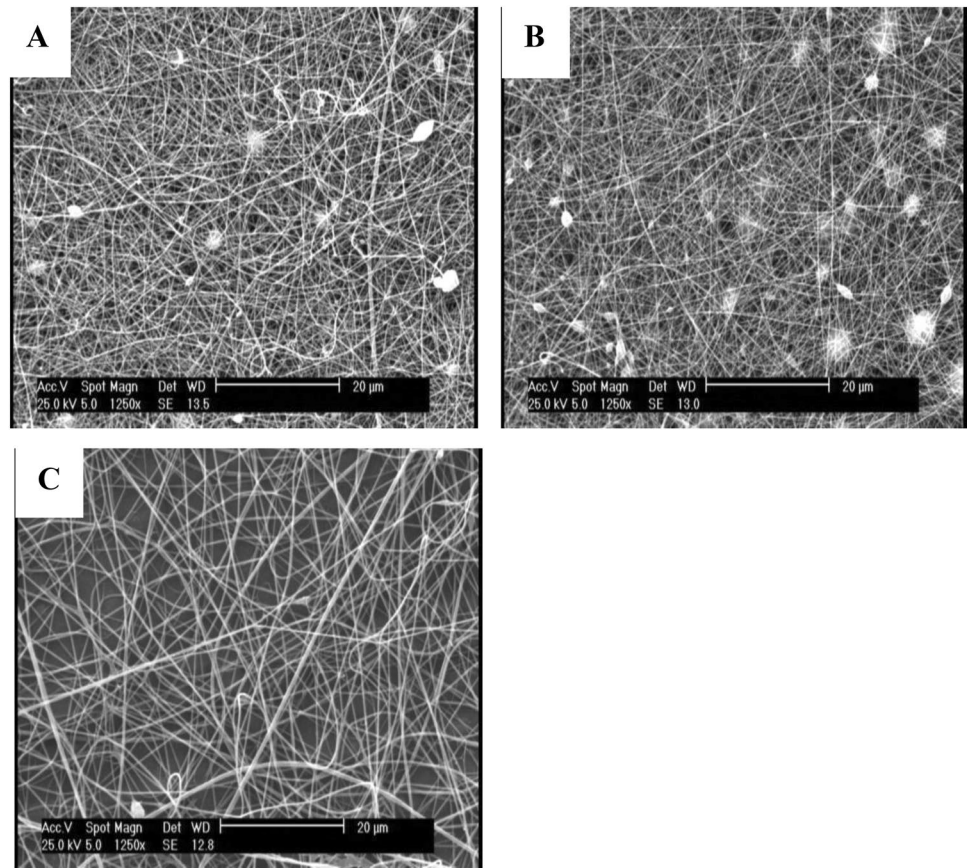
Cellular toxicity, proliferation and morphological study

MTT assay was employed for cellular toxicity evaluation. To the preparation of samples for this analysis, fiber mats were sterilized by submerging in ethanol (70 (%v/v)) for 30 min

and exposure to UV light for 15 min. PC12 cells with a density of 5000 cells/cm² were cultured on fibrous nanofibers and a multiwell culture plate as a control sample. The cellular viability was determined with MTT assay during 24 and 48 h. Briefly, 100 μl of culture medium with 10 μl of MTT were added to specimens and incubated for 2 h. After color change observation, 100 μl DMSO was added to each well and kept at dark conditions. Cellular absorbance was measured at 570 nm using an ELISA reader. All cellular culture analyses were repeated three times.

For cellular morphology observation using SEM device (ZEISS, Sigma VP), cultured cells were fixed with 2.5% glutaraldehyde for 2 h and soaked in gradient ethanol concentrations for 50 min. Finally, the prepared samples with coated with a thin layer of gold for SEM analysis.

Fig. 3 SEM micrograph of **A** GC1, **B** GC2, **C** GC3 nanofibers



Statistics

One-way ANOVA by Graph-Pad software, USA was used to compare the results. A significant difference was reported in p value < 0.05 .

Results and discussion

PVDF-chitosan–gelatin nanofiber analyses

In the present study, piezoelectric nanofibers comprising PVDF-chitosan–gelatin were synthesized using the dual-electrospinning method. Figures 2 and 3 represent the morphology of PVDF and PVDF-chitosan–gelatin nanofibers, respectively. In these images, the effect of PVDF concentration on synthesized nanofibers was studied. The morphology of electrospun nanofibers in the lower concentrations [5, 7, and 10 (%w/v)] indicates that the fibrous fibers with free beads structures have not been formed. The concentration of 25 (%w/v) has been induced ribbon-like morphology to nanofibers structures and 15 (%w/v) of this polymer has caused fibrous structures with ultrafine morphology which is due to an appropriate viscosity and surface tension of this polymer solution. In principle, concentration and viscosity

are the decisive factors in nanofiber synthesis (Bayat and Ahamd Ramazani 2020). PVDF nanofibers at the concentration of 15 (%w/v) with an appropriate viscosity led to uniform piezoelectric nanofibers.

The PVDF-chitosan–gelatin nanofibers were synthesized using two nozzle electrospinning method. At this experimental section, 15 (%w/v) of PVDF solution was set as the optimum concentration of PVDF. The SEM micrographs of PVDF-chitosan–gelatin nanofibers as a function of three ratios are shown in Fig. 3. In GC1, fiber-beads with fused fibers were created but with a decrease in chitosan concentration, ultrafine nanofibers with uniform morphology were observed in GC3. Morphology of GC3 in SEM analysis indicates that with the variation of chitosan–gelatin concentration the structure of fiber formed has been turned. Therefore, in GC3, PVDF-chitosan–gelatin has made a suitable viscosity and electrical conductivity to the successful electrospinning process compared to other proportion of chitosan–gelatin at the constant electrospinning parameters (Fig. 3). For further study, the GC3 sample was selected. by raising the volume ratio of gelatin in chitosan–gelatin composition, the uniformity of nanofibers has been improved and the average fiber diameter showed a decrement trend. This is due to the present high level of gelatin polymeric chains and reducing the repulsive forces within the charged polymeric chains in

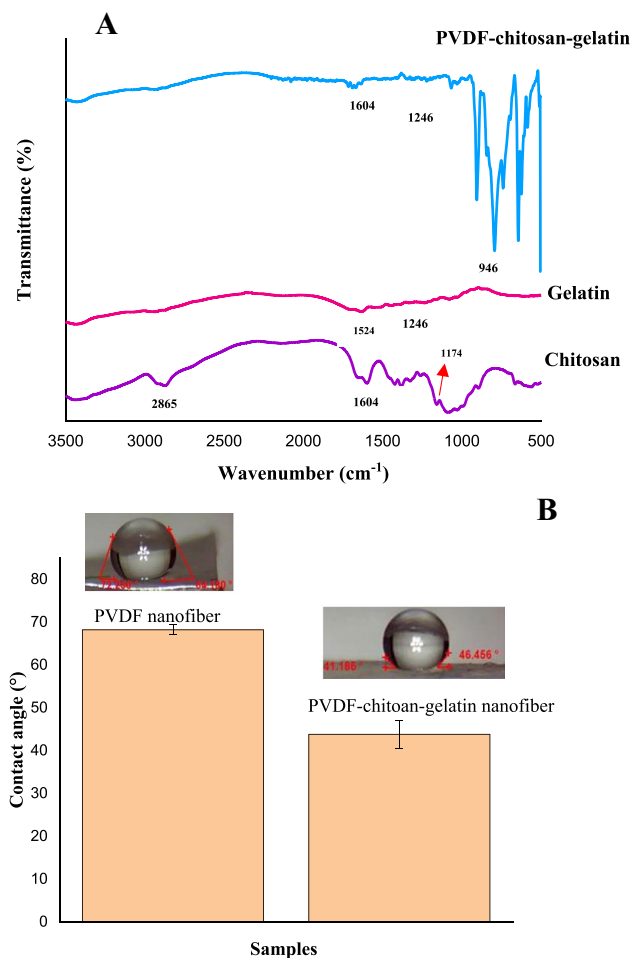


Fig. 4 PVDF-chitosan-gelatin nanofibers, **A** FTIR spectra of chitosan, gelatin and chitosan-gelatin nanofibers, **B** Contact angle of synthesized nanofibers

the obtained solution. Generally, solution conductivity and viscosity play a critical role in fiber morphology and diameter. In the sample with a higher ratio of gelatin in PVDF-chitosan-gelatin nanofibers, more uniformity and less fiber diameter were apperceived.

The synthesis of PVDF-chitosan-gelatin nanofibers was confirmed with the help of FTIR spectra. As shown in Fig. 4A, the detected vibration bands which are associated with chitosan are 2865 cm^{-1} (CH_2 stretching), 1174 cm^{-1} (C-O-C stretching), 1604 cm^{-1} (C=O stretching). In gelatin spectrum vibration bands of CH_2 symmetric stretch, Amid II and Amid III at wavenumbers of 2850 cm^{-1} , 1524 cm^{-1} , and 1246 cm^{-1} were figured out respectively. CH_2 and CF_2 in PVDF-chitosan-gelatin nanofibers were detected at 946 and 598 cm^{-1} attributed to PVDF polymers and vibration band at 1246 cm^{-1} as a clue of gelatin presence and 1604 cm^{-1} confirmed the successful electrospinning of PVDF-chitosan-gelatin nanofibers.

The wettability traits of self-electrical electrospun nanofibers were examined with a contact angle analyzer. Generally, PVDF has hydrophobic nature and the co-presence of chitosan-gelatin in the synthesized nanofibers has decreased the contact angle of fibers which makes possible the tendency to improve the hydrophilicity of nanofibers. The confirmation of improved wettability in PVDF-chitosan-gelatin is clued with the degree of contact angle in neat PVDF nanofibers with the number of 68.23° and 43.82° for PVDF-chitosan-gelatin. The contact angle results are shown in Fig. 4B. This reduction in the contact angle of fiber mats in PVDF-chitosan-gelatin is originated from the functionality of chitosan and gelatin in the structure of PVDF-chitosan-gelatin nanofibers.

PAG analyses

Synthesis of PAG nanocomposite was studied with FTIR and XRD as shown in Fig. 5A and B. In the FTIR of graphene and PAG, the specific vibration bands describe the prosperous polymerization of aniline with the mechanism of emulsion polymerization. The N-H stretching band at 3400 cm^{-1} and the stretching C-N bands of the benzenics and quinonics rings in the range of $1500\text{--}1600\text{ cm}^{-1}$ were detected, also deprotonation of structure using delocalization of electrical charge was clued with the peak of 1128 cm^{-1} . Electron delocalization is the main mechanism of enhanced electrical conductivity of PAG and this point is revealed through the promotion of quinoid against benzoid rings.

XRD patterns in Fig. 5B illustrate a strong and sharp peak at $2\Theta = 24\text{--}26^\circ$ attributed to graphene nanosheets. In the XRD of the PAG profile, the diffraction peak at $2\Theta = 20^\circ$ is responsible for the isomorphous structure due to polyaniline chains in the PAG composite. Reduction in intensity of the diffracted peak of graphene and also the appearance of new peaks in the range of $2\Theta = 5\text{--}25^\circ$ supports the claim of PAG synthesis.

For morphological characterization of graphene and PAG nanoparticles, SEM analysis was performed. According to the obtained results shown in Fig. 5C, during emulsion polymerization of aniline, sheet-based graphene nanoparticles were covered which is in agreement with other reports (Bayat and Ahamd Ramazani 2020) (Figs. 6 and 7).

Morphology of gellan gel

Structural analysis

To evaluate the structural analysis of gellan gel containing PAG nanocomposite, XRD patterns were studied. As shown in Fig. 8, the diffraction peaks related to PAG

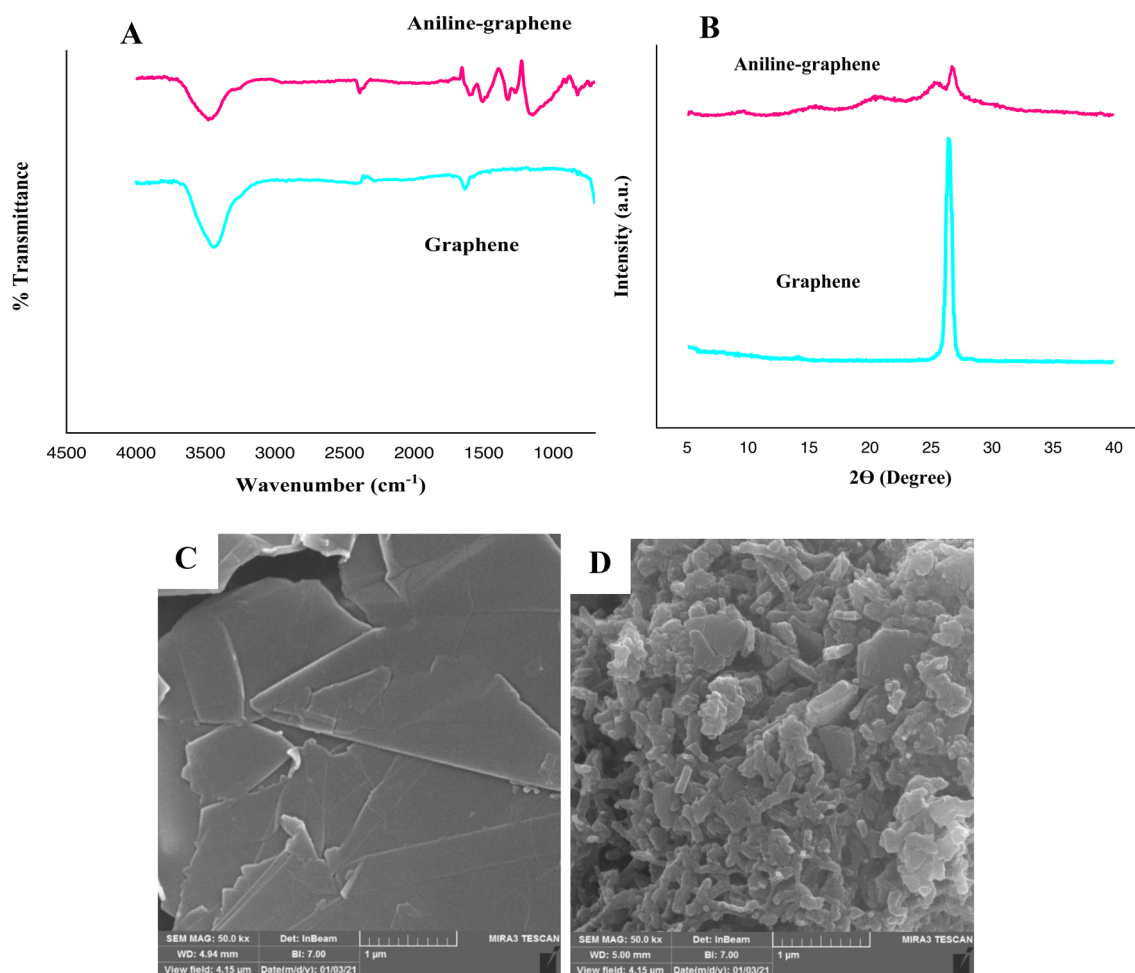


Fig. 5 Chemical and structural analyses of PAG nanocomposite; **A** FTIR spectra, **B** XRD and SEM images of **C** graphene, **D** PAG nanocomposite

particles ($2\theta = 24\text{--}26^\circ$ and $2\theta = 5\text{--}10^\circ$) were detected in the XRD graph of gellan PAG. The partial enhancement of the peak intensity in composite compare to pure gellan scaffold is because of the graphene sheets in the PAG structure. XRD pattern of gellan nanocomposite suggests that incorporation of PAG nanocomposites between gellan polymeric chains, engendered to increase the level of crystallinity and gellan PAG has more crystalline phase compare to neat gellan. This increment in the intensity of gellan-PAG nanocomposite confirmed the modification of gellan with PAG.

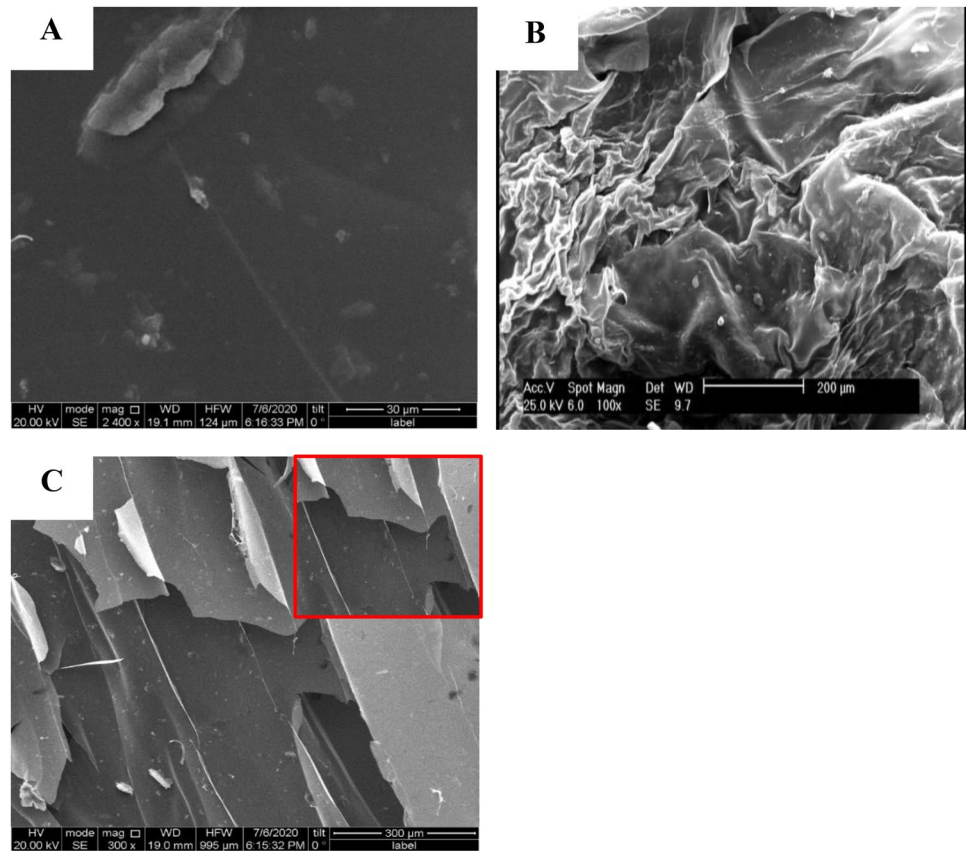
Gelation time

The inverted tube was the method to determine the gelation time. In the gellan polymer, the gel is formed with physically

bonded to each other (Yang et al. 2019). Placement of any fillers in between the gellan polymeric chains is an effective factor that can control the gelation time and temperature as two critical factors in the use of in-situ gel applications.

Based on our examination, to create the stable gellan gel the approximately time of 4 min is required. In Fig. 9 the alteration time for completion of the gelation process is plotted. The presence of PAG engendered to increase the gelation time to 6.5 min. The incorporation of these conductive particles in the structure of polymer causes the entanglement process of these chains to be delayed and the gelation time to change. The positioning of PAG particles in the polymer eliminates enough space for a physical connection between the chains.

Fig. 6 SEM image of **A** PAG in gellan gel, **B** gellan gelation through direct freezing, **C** gellan scaffold with PAG particles



Rheology

The rheological behavior of gellan gel containing different amounts of PAG particles was evaluated and viscosity, storage modulus (G'), and loss modulus (G'') results of these samples are shown in Fig. 10. In the study of rheological behavior, G' and G'' depict linear behavior and toughening trend in gel with an increase of PAG concentration. With the increase of PAG loading in gellan, ameliorated storage and loss modulus of gellan samples was comprehended. Gellan gel toughening using embedding PAG particles was observed in the rheological examination. The existence of particles between polymeric chains in gellan structure can make a partially cross-link among chains (Li et al. 2020).

The regime behavior of G' , G'' has linear behavior and toughening trend in gel with an increase of PAG concentration was obtained. Placement of particles between gellan polymer chain induced the improve the mechanical traits of gellan-based composite. The existence of particles between polymeric chains in gellan structure can make a partially cross-link among chains (Mohseni et al. 2016). Based on rheology results, gel toughening using PAG particles is because of the energy adsorbing through particles (Flávia Souza Almeida 2019).

Electrical properties

The electrical conductivity of substrates is one of the recognized requirements of the neural scaffolds which can accelerate nerve regeneration using degradable scaffolds (Yaobin et al. 2016). Diverse conductive materials including poly aniline demonstrated their potential for neurite outgrowth (Wang et al. 2019; Guo and Ma 2018). But control the electrical activity of synthesized piezoelectric NGC and ameliorate this potential based on tissue requirement, pushed researchers to synthesize novel nanocomposites such as PAG. According to Table 2, the electrical conductivity of gellan-based nanocomposite was ascended with the PAG concentration. The electrical conductivity of scaffolds from 0 without any PAG loading has ascended to 10.1×10^{-5} with the particle loading of 2 (wt.%) and these results exhibited the relationship between PAG loading and electrical conductivity. The procured conductivity in the mentioned conduit is on modification of graphene with aniline and also proper diffusion in the polymeric matrix.

Fig. 7 Morphology of gellan gel **A** without insulation, **B** insulation with the thickness of 15 mm, **C** insulation with the thickness of 25 mm

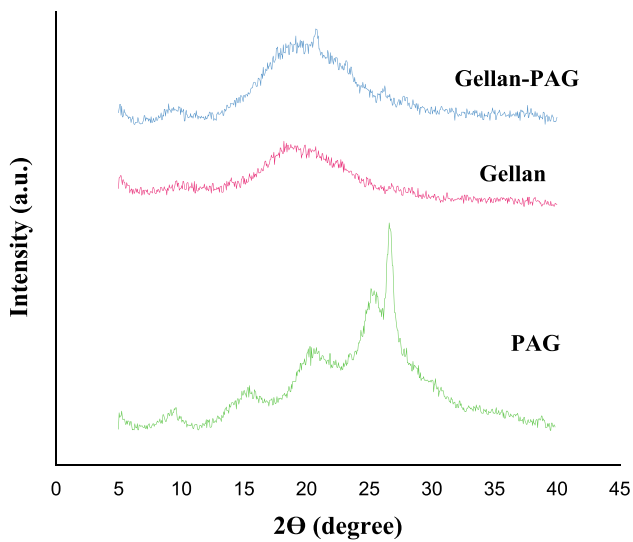
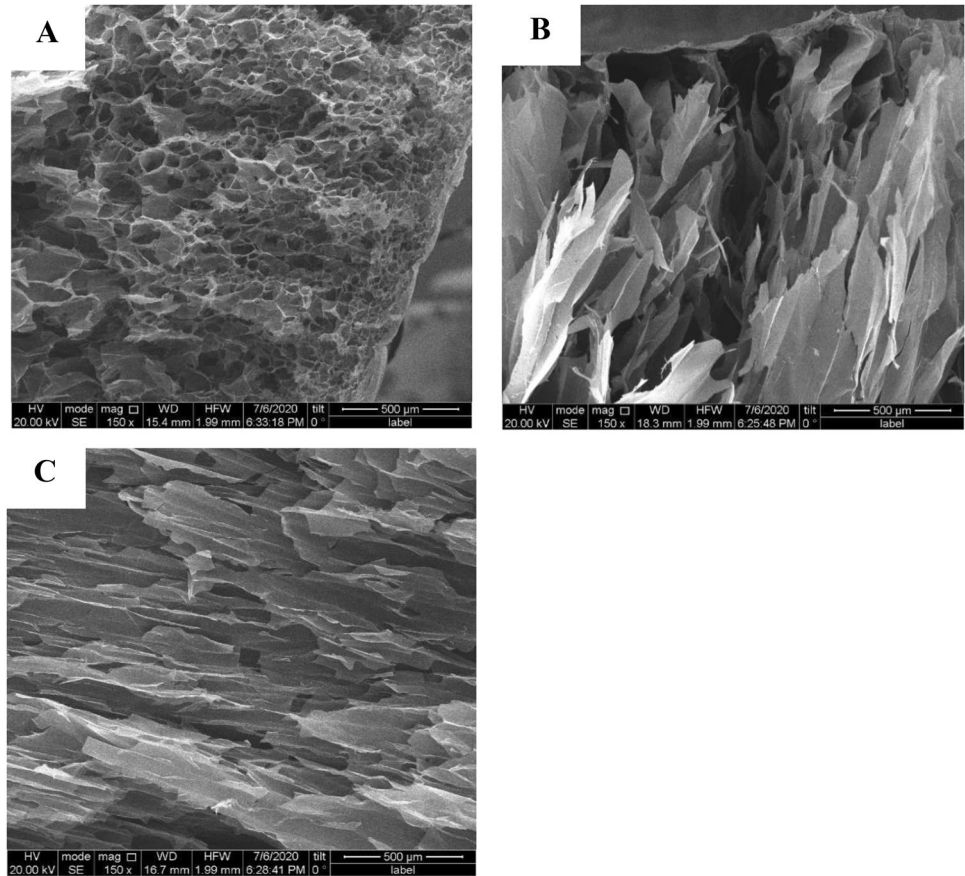


Fig. 8 XRD patterns of gellan and gellan PAG; XRD illustrates the increase of crystallinity compared to pure gellan

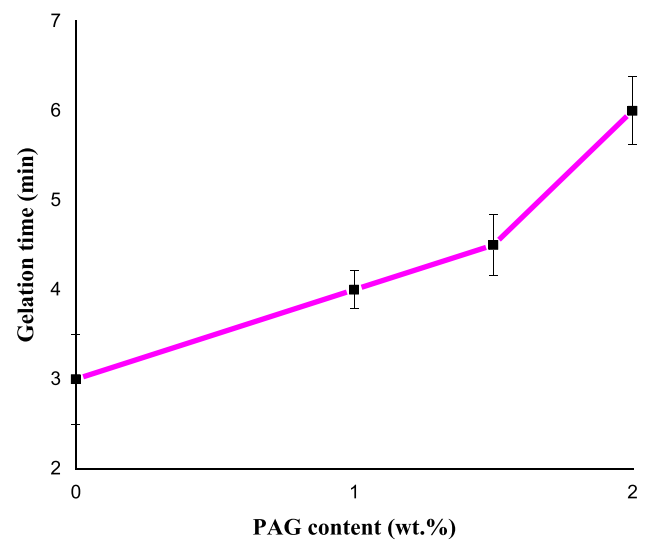


Fig. 9 Gelation time of gellan-based nanocomposite with different concentration of PAG

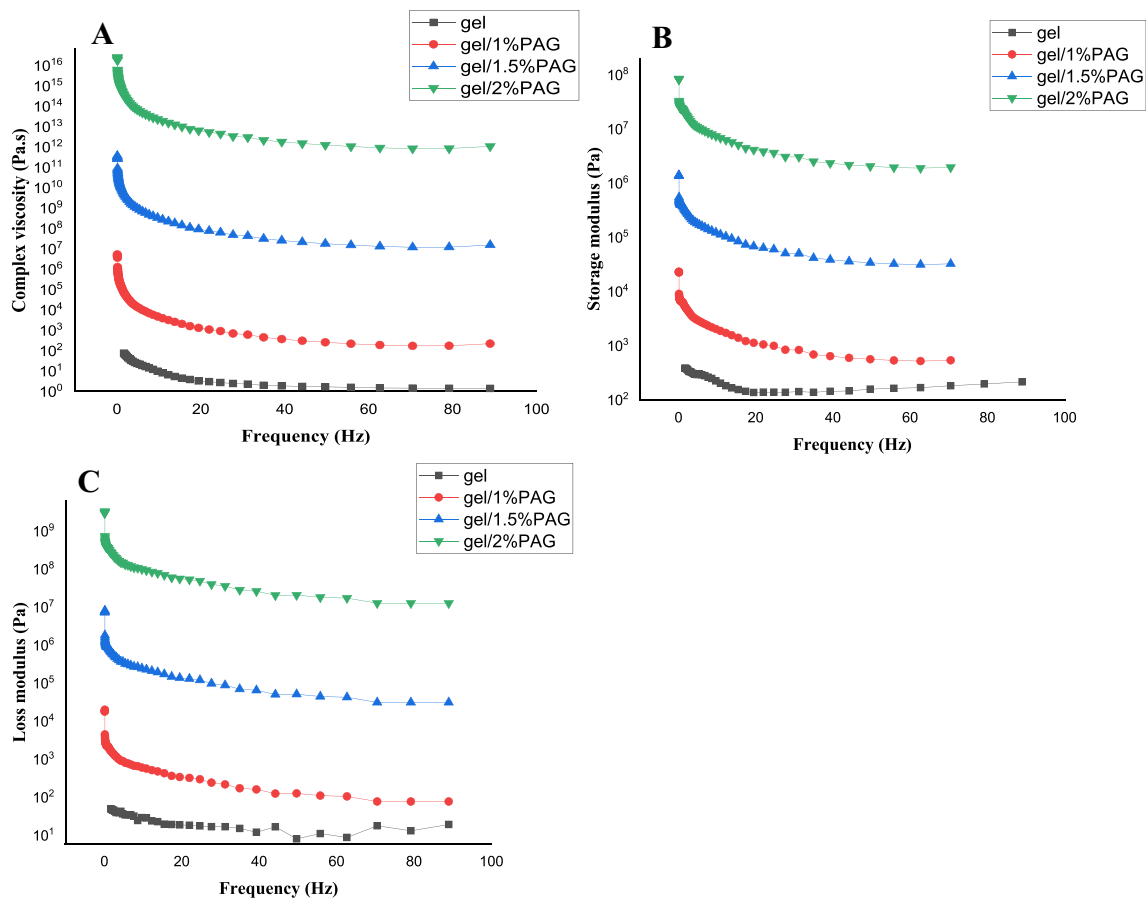


Fig. 10 Rheological results of gellan PAG; **A** complex viscosity, **B** storage modulus, **C** loss modulus

Conduit characterization

Biodegradation assessment of scaffolds was performed with weight loss. Ideal scaffolds should have a degradation rate in accordance with the native tissue (Sathain et al. 2021). As shown in Fig. 11A, the degradation trend of scaffolds has altered with various concentration of PAG. The scaffold with 0 (wt.%) PAG retained its stability in PBS solution for 30 days and only 3% of the scaffold degraded. PAG particle loading caused the decrementing behavior in these samples. In the PAG, crystalline nature can have an effective role to control the degradation behavior. Reduce the degradation

rate in structure by 2 (wt.%) PAG is reasonable with the high loading of PAG. Immersion of gellan nanocomposite in PBS resulted from the dehydration of the gel. In the PBS, the ionic concentration is higher than that of the hydrogel. Localized the PAG particle in the polymer chain with the crystalline structure leads to slower degradation of gellan-based substrate.

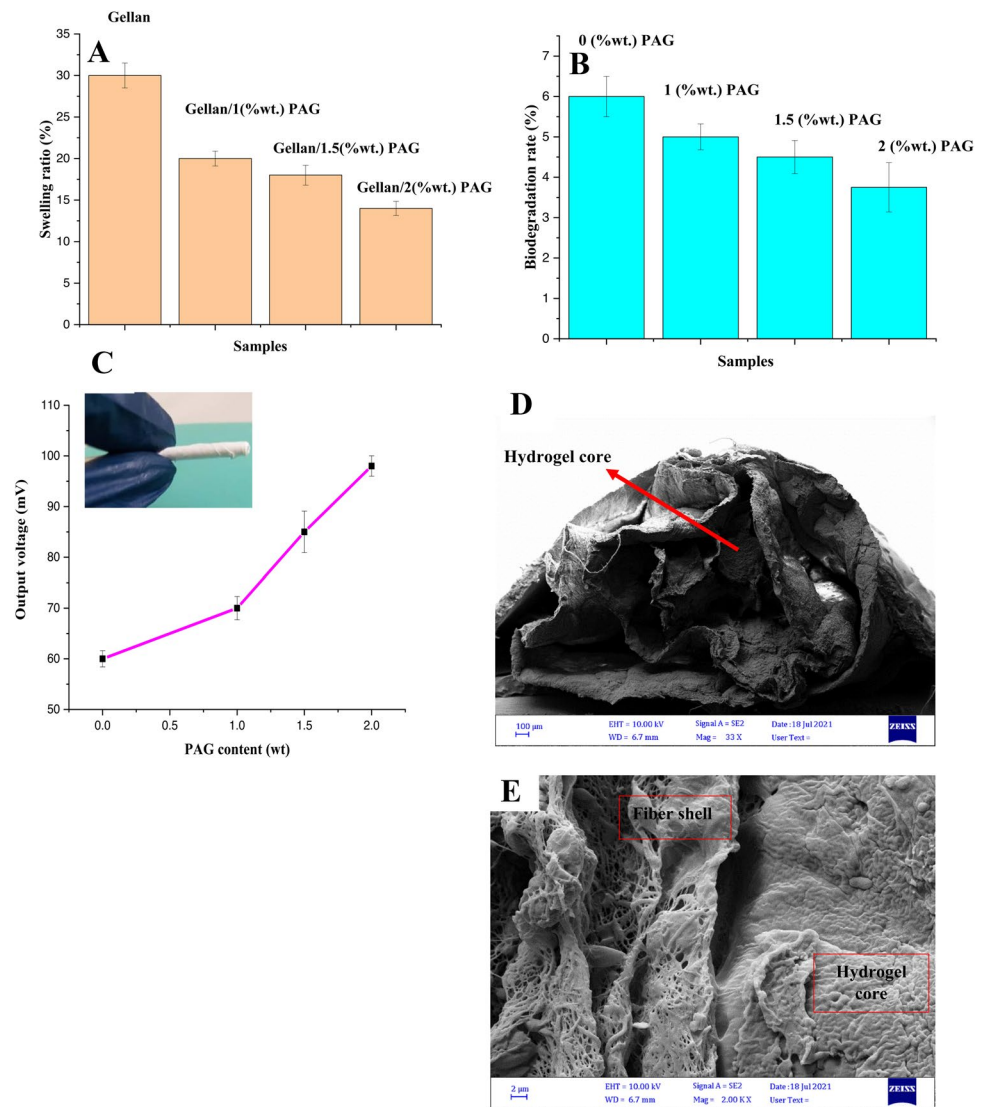
The graphs of the swelling ratio of pure gellan scaffold and filled with PAG particles are shown in Fig. 11B. In all diagrams within the first 10 h, ascending slope of swelling was observed. After this time, swelling reaches a steady state. But the incorporation of PAG in gellan solution undergo different swelling ration in the nanocomposite. In PAG nanocomposite, two aspects of the amorphous and crystalline nature of polyaniline and graphene are received. Changes in the swelling trend of samples loaded PAG show diverse swelling behavior as a result of the presence two-part of PAG in gellan scaffold.

In this study, a self-electrical substrate was fabricated as a possible candidate for neural conduits. For this aim, PVDF-based nanofiber was designed, and also the synthesized PAG nanostructures were designed as a synergic agent.

Table 2 Electrical conductivity of gellan containing different amount of PAG

Sample	Electrical conductivity (S/cm)
0	0
1	7.8×10^{-5}
1.5	9.5×10^{-5}
2	12×10^{-5}

Fig. 11 Conduit properties study; **A** swelling trend of samples with varied concentration of PAG, **B** biodegradation of specimens containing 1, 1.5 and 2 (wt.%) PAG, **C** output voltage of piezoelectric neural conduit, **D** SEM image of core–shell conduit, **E** Interface image of hydrogel core and fiber shell



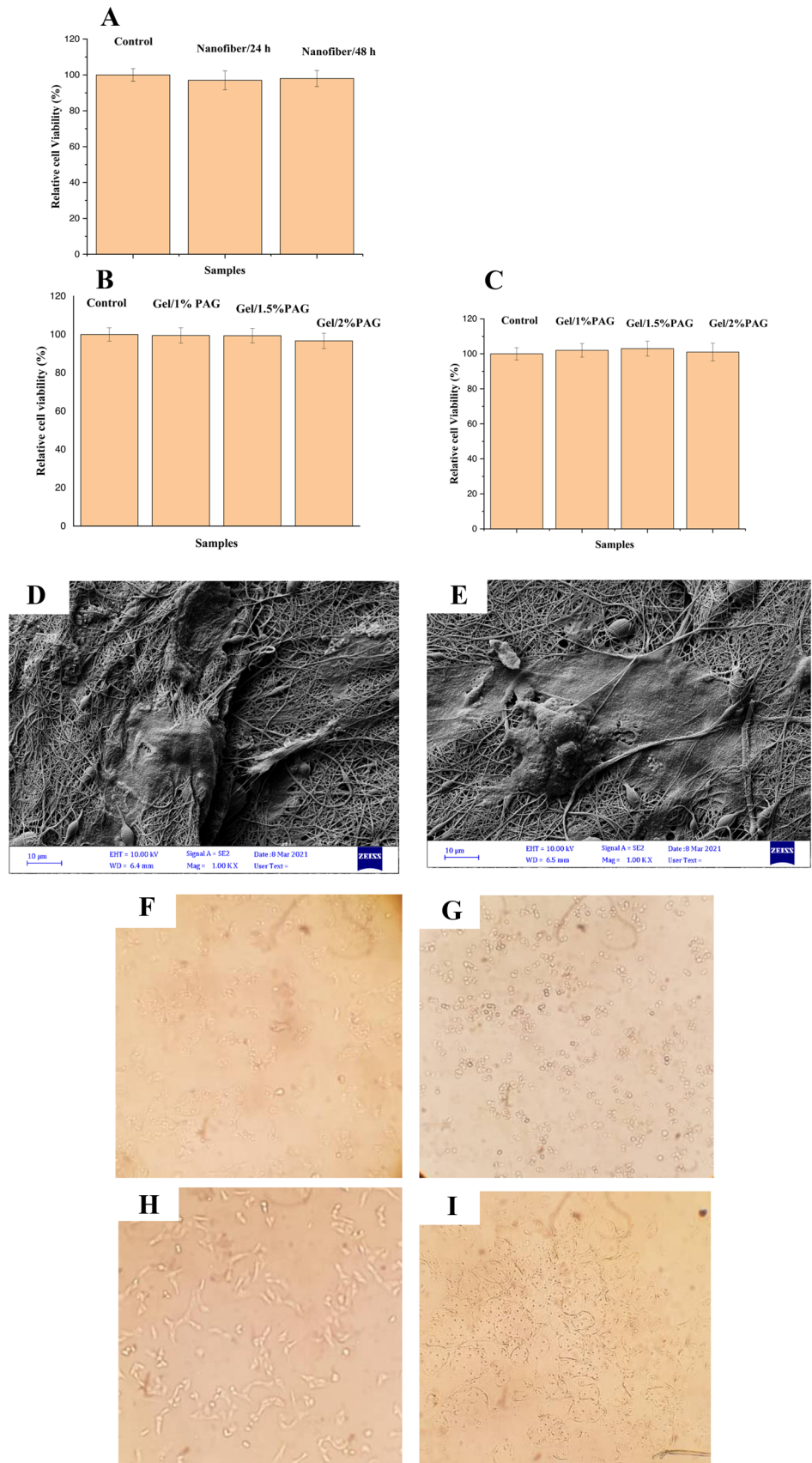
The output voltage of the neural conduit as a function of PAG loading was recorded with the use of a digital oscilloscope and plotted in Fig. 11C. The piezoelectric test reveals that the neural conduit has a piezoelectric feature and the obtained voltage has an increment trend with the change of PAG concentration. Figure 11 provided sufficient evidence to confirm the idea of embedding conductive particles to manipulate the output voltage. Based on these results, conductive PAG particles engendered to enhance output voltage with the localized electrical voids in the presence of piezoelectric fibers (Chen et al. 2020).

The core–shell morphology of the conduit was characterized using SEM analysis in Figs. 11D, E. Incorporation of conductive in-situ gellan in the core of neural conduit is observed in Fig. 11D and also the interface of fiber shell and hydrogel core in Fig. 11E represent the stable complex of core–shell structure.

In vitro biocompatibility evaluation

PC12 cells were selected as a model of neural cells for cytocompatibility appraisal in neural conduit for peripheral nerve regeneration. MTT assay was conducted for toxicity study and as plotted results shown in Fig. 12, electrospun fibrous nanofibers didn't have any specific toxicity for cultured cells and in the period of 48 h, increase the cellular viability is attributed to enhance the proliferation of PC12 cells. An appropriate interaction between the cellular ECM and piezoelectric nanofibers is the basic reason for the cellular tendency to proliferation. In synthesized nanofibers, the presence of chitosan and also gelatin with the specific active site for cellular ligands prepare a proper micro-environment for sufficient cellular interactions (Olad and Hagh 2019). Gellan-PAG cellular viability showed acceptable cellular compatibility. In the gellan sample containing 2 (wt.%) PAG

Fig. 12 Cellular study of samples; **A** MTT of PVDF-chitosan-gelatin nanofibers, **B** MTT assay of gellan containing different content of PAG during 24 h, **C** MTT of gellan PAG with diverse content of PAG for 4 h, **D** cell morphology of PVDF-chitosan-gelatin for 24 h, **E** cellular attachment of PC12 on PVDF-chitosan-gelatin for 48 h, **E** cellular observation of gellan, **F** gellan-1 (wt.% PAG, **G** gellan-1.5 (wt.%) PAG, **H** gellan-2 (wt.%)



minor decrement trend of PC12 viability was observed. A higher amount of poly aniline is responsible for this phenomenon (Mohammed et al. 2020). But this alteration in cellular viability is not specific and can be considered as a biocompatible substrate. Compared to another study with the focus of using conductive structure to control the PC12 cellular alignment and attachment, the acceptable reaction of neural cells with conductive structures is expected (Yaobin et al. 2018).

Cellular morphology of PC12 cultured cell in Fig. 12C, attached cells on piezoelectric nanofibers is confirmed and support in terms of cellular attachment and proliferation of PC12.

Conclusion

In this study, a self-electrical PVDF-chitosan–gelatin conduit filled with gellan nanocomposite was fabricated. For this purpose, piezoelectric nanofibers were synthesized using the dual-electrospinning method. The conductivity of the specimen was supplied using poly aniline-graphene with the conductivity of $12 \times 10^{-5} \text{ S cm}^{-1}$. The output voltage of self-electrical based nan-conduit was improved with the synergic effect of conductive particles and the electro-mechanical features of the designed conduit have proved the sufficient requirements of novel self-electrical conduit for neural regeneration.

Declarations

Conflict of interest We declare that we don't have any conflict of interest.

References

- Abnoos M, Mohseni M, Mousavi SAJ, Ashtari K, Ilka R, Mehravi B (2018) Chitosan-alginate nano-carrier for transdermal delivery of pirfenidone in idiopathic pulmonary fibrosis. *Int J Biol Macromol* 118:1319–1325
- Almeida FS, Sato AC (2019) Structure of gellan gum–hydrolyzed collagen particles: effect of starch addition and coating layer. *Food Res Int* 121:394–403
- Badatya S, Kumar A, Sharma C, Srivastava AK, Chaurasia JP, Gupta MK (2021) Transparent flexible graphene quantum dot-(PVDF-HFP) piezoelectric nanogenerator. *Mater Lett* 290:129493
- Bayat A, Ramazani SAA (2021) Biocompatible conductive alginate/polyaniline-graphene neural conduits fabricated using a facile solution extrusion technique. *Int J Polymer Mater Polymer Biomater* 70(7):486–495
- Bhattacharai DP, Shrestha S, Shrestha BK, Park CH, Kim CS (2018) A controlled surface geometry of polyaniline doped titania nanotubes biointerface for accelerating MC3T3-E1 cells growth in bone tissue engineering. *Chem Eng J* 350:57–68
- Chen C, Bai Z, Cao Y, Dong M, Jiang K, Zhou Y, Tao Y, Gu S, Xu J, Yin X, Xu W (2020) Enhanced piezoelectric performance of BiCl₃/PVDF nanofibers-based nanogenerators. *Compos Sci Technol* 192:108100
- Farooqi BA, Yar M, Ashraf A, Farooq U, Ayub K (2020) Graphene-polyaniline composite as superior electrochemical sensor for detection of cyano explosives. *Eur Polymer J* 135:109981
- Gao F, Mu J, Bi Z, Wang S, Li Z (2021) Recent advances of polyaniline composites in anticorrosive coatings: a review. *Prog Org Coat* 151:106071
- Guo B, Ma PX (2018) Conducting polymers for tissue engineering. *Biomacromol* 19:1764–1782
- Gupta D, Tator CH, Shoichet MS (2006) Fast-gelling injectable blend of hyaluronan and methylcellulose for intrathecal, localized delivery to the injured spinal cord. *Biomaterials* 27:2370–2379
- Hsueh YY, Chang YJ, Huang TC, Fan SC, Wang DH, Chen JJ, Wu CC, Lin SC (2014) Functional recoveries of sciatic nerve regeneration by combining chitosan-coated conduit and neurosphere cells induced from adipose-derived stem cells. *Biomaterials* 35(7):2234–2244
- Hua Wu, Fang Q, Liu J, Xiaofeng Yu, Yigui Xu, Wan Y, Xiao Bo (2018) Multi-tubule conduit-filler constructs loaded with gradient-distributed growth factors for neural tissue engineering applications. *J Mech Behav Biomed Mater* 77:671–682
- Ilka R, Mohseni M, Kianirad M, Naseripour M, Ashtari K, Mehravi B (2018) Nanogel-based natural polymers as smart carriers for the controlled delivery of timolol maleate through the cornea for glaucoma. *Int J Biol Macromol* 109:955–962
- Jun I, Jeong S, Shin H (2009) The stimulation of myoblast differentiation by electrically conductive sub-micron fibers. *Biomaterials* 30:2038–2047
- Kung CY, Wang TL, Lin HY, Yang CH (2021) A high-performance covalently bonded self-doped polyaniline–graphene assembly film with superior stability for supercapacitors. *J Power Sources* 490:229538
- Lee S, Choi JH, Park A, Rim M, Youn J, Lee W, Song JE, Khang G (2020) Advanced gellan gum-based glycol chitosan hydrogel for cartilage tissue engineering biomaterial. *Int J Biol Macromol* 158:452–460
- Li M, Zhang P, Zhang D (2018) PVDF piezoelectric neural conduit incorporated pre-differentiated adipose-derived stem cells may accelerate the repair of peripheral nerve injury. *Med Hypothesis* 114:55–57
- Li A, Gong T, Li X, Li X, Yang Xi, Guo Y (2020) Preparation of thermally stable emulsion gels based on glucono-δ-lactone induced gelation of gellan gum. *Int J Biol Macromol* 156:565–575
- Lin C-C, Chiu J-Y (2020) A novel γ-PGA composite gellan membrane containing glycerol for guided bone regeneration. *Mater Sci Eng C* 118:11404
- Liu S, Sun L, Zhang H, Qingxi Hu, Wang Y, Ramalingam M (2020) High-resolution combinatorial 3D printing of gelatin-based biomimetic triple-layered conduits for nerve tissue engineering. *Int J Biol Macromol* 166:1280–1291
- Magaz A, Li X, Gough JE, Blaker JJ (2021) Graphene oxide and electroactive reduced graphene oxide-based composite fibrous scaffolds for engineering excitable nerve tissue. *Mater Sci Eng C* 119:111632
- Maharjan B, Kaliannagounder VK, Jang SR, Awasthi GP, Bhattacharai DP, Choukrani G, Park CH, Kim CS (2020) In-situ polymerized polypyrrole nanoparticles immobilized poly(ε-caprolactone) electrospun conductive scaffolds for bone tissue engineering. *Mat Sci Eng C* 114:111056
- Maity P, Sen IK, Chakraborty I, Mondal S, Bar H, Bhanja SK, Mandal S, Maity GN (2021) Biologically active polysaccharide from edible mushrooms: a review. *Int J Biol Macromol* 172:408–417

- Mohammadi M, Ramazani SaadatAbadi A, Mashayekhan S, Sanaei R (2020) Conductive multichannel PCL/gelatin conduit with tunable mechanical and structural properties for peripheral nerve regeneration. *J Appl Polym Sci* 137:49219
- Mohammed M, Mekala LP, Chintalapati S, Chintalapati VR (2020) New insights into aniline toxicity: aniline exposure triggers envelope stress and extracellular polymeric substance formation in *rubrivivax benzoatilyticus* JA2. *J Hazard Mater* 385:121571
- Mohseni M, Dezfouli Z (2020) Flake-like glass nanoparticles reinforced natural polymeric scaffold as a promising substrate for bone regeneration. *J Polym Res* 27:1–10
- Mohseni M, Atai M, Sabet A, Beigi S (2016) Effect of plate-like glass fillers on the mechanical properties of dental nanocomposites. *Iran Polym J* 25:129–134
- Mohseni M, Shojaei S, Mehravi B, Mohammadi E (2020) Natural polymeric nanoparticles as a non-invasive probe for mesenchymal stem cell labelling. *Artif Cells Nanomed Biotechnol* 48:770–776
- Mohseni M, Ramazani SAA, Farshad H, Nemati NH (2021a) Gelatin gel comprising short PVDF based-nanofibers: the effect of piezoelectric nanofiber on the mechanical and electrical behavior. *Mater Today Commun* 26:101785
- Mohseni M, Ramazani SA, Shirazi FH, Nemati NH (2021b) Preparation and characterization of self-electrical stimuli conductive gelatin based nano scaffold for nerve regeneration containing chopped short spun nanofibers of PVDF/MCM41 and polyaniline/graphene nanoparticles: physical, mechanical and morphological studies. *Int J Biol Macromol* 167:881–893
- Olad A, Hagh HBK (2019) Graphene oxide and amin-modified graphene oxide incorporated chitosan-gelatin scaffolds as promising materials for tissue engineering. *Compos B Eng* 162:692–702
- Pan L, Cai C, Liu C, Liu Di, Li G (2021) Recent progress and advanced technology in carbohydrate-based drug development. *Curr Opin Biotechnol* 69:191–198
- Park H, Kim H, Kim GY, Lee MY, Kim Y, Kang S (2021) Enhanced biodegradation of hydrocarbons by *pseudomonas aeruginosa*-encapsulated alginate/gellan gum microbeads. *J Hazard Mater* 406:124752
- Sathain A, Monvisade P, Siriphannon P (2021) Bioactive alginate/carrageenan/calcium silicate porous scaffolds for bone tissue engineering. *Mater Today Commun* 26:102165
- Shen C-C, Yang Y-C, Liu B-S (2011) Large-area irradiated low-level laser effect in a biodegradable nerve guide conduit on neural regeneration of peripheral nerve injury in rats. *Injury* 42:803–813
- Silva D, de Sousa HC, Gil MH, Santos LF, Oom MS, Alvarez-Lorenzo C, Saramago B, Serro AP (2021) Moxifloxacin-imprinted silicone-based hydrogels as contact lens materials for extended drug release. *Eur J Pharm Sci* 156:105591
- Wang L, Yaobin Wu, Tianli Hu, Ma PX, Guo B (2019) Aligned conductive core-shell biomimetic scaffolds based on nanofiber yarns/hydrogel for enhanced 3D neurite outgrowth alignment and elongation. *Acta Biomater* 96:175–187
- Xiao J, Ma Y, Wang W, Zhang K, Tian X, Zhao K, Duan S, Li S, Guo Y (2021) Incorporation of gelatin improves toughness of collagen films with a homo-hierarchical structure. *Food Chem* 345:128802
- Yang Xi, Hou Y, Gong T, Sun L, Xue J, Guo Y (2019) Concentration-dependent rheological behavior and gelation mechanism of high acyl gellan aqueous solutions. *Int J Biol Macromol* 131:959–970
- Yaobin Wu, Wang L, Guo B, Shao Y, Peter XM (2016) Electroactive biodegradable polyurethane significantly enhanced Schwann cells myelin gene expression and neurotrophin secretion for peripheral nerve tissue engineering. *Biomaterials* 87:18–31
- Yaobin Wu, Wang L, Tianli Hu, Ma PX, Guo B (2018) Conductive micropatterned polyurethane films as tissue engineering scaffolds for schwann cells and PC12 cells. *J Colloids Interface Sci* 518:252–262
- Zeng C, Sheng P, Xie G, Zhu J, Dong P, Quan D (2011) Fabrication of PLLA nanofibrous multi-channel conduits for neural tissue engineering. *J Control Release* 152:234
- Zhang M, Zhao X (2020) Alginate hydrogel dressings for advanced wound management. *Int J Biol Macromol* 162:1414–1428

Publisher's Note Springer Nature remains neutral with regard to jurisdictional claims in published maps and institutional affiliations.